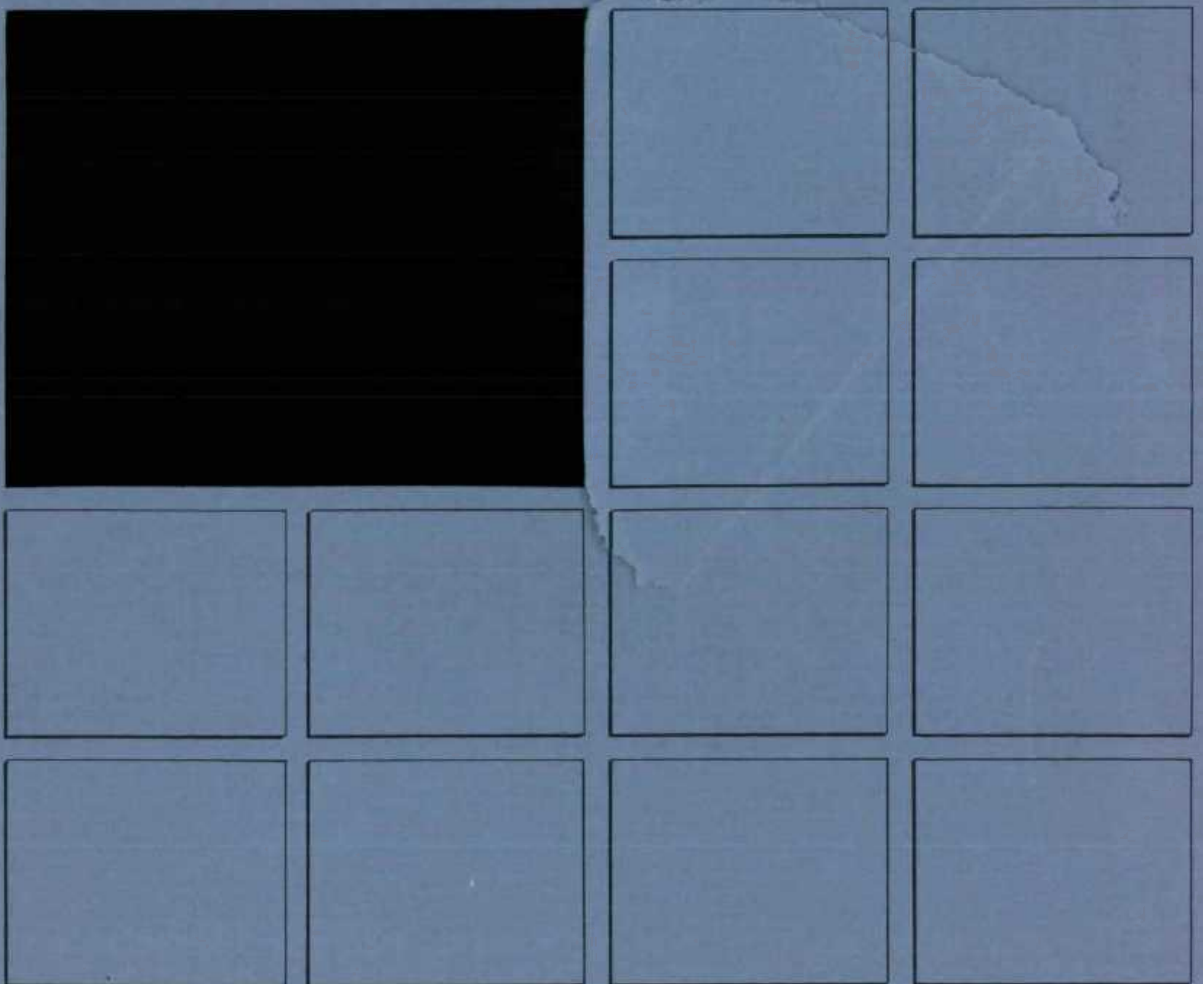




INSTITUTE of
HYDROLOGY



THE FLOW OF GROUNDWATER
IN A COASTAL AQUIFER

R. S. WIKRAMARATNA

THE FLOW OF GROUNDWATER IN A COASTAL AQUIFER

R.S. WIKRAMARATNA
INSTITUTE OF HYDROLOGY
WALLINGFORD
OXON

A dissertation submitted to the University
of Reading in partial fulfillment of the
requirements for the degree of Master of
Science.

Department of Mathematics, University of
Reading.

September 1981

Summary

The Galerkin finite element method is used to solve the coupled equations governing the steady-state flow of groundwater and the dispersion of salt in a coastal aquifer using an iterative scheme which can be applied either to confined or unconfined aquifers. The effects of both molecular diffusion and mechanical dispersion are included in the model.

The method is applied to a test problem based on the Mogadishu coastal plain in Somalia. Solutions are obtained both for the salt concentration and the flow velocities in a vertical section of the aquifer perpendicular to the coast. The effects, both on these solutions and on the rates of convergence, of altering the diffusion and dispersion parameters are investigated.

CONTENTS

Page no:

Introduction

Equations and Boundary Conditions

- | | | |
|-----|-----------------------------------|----|
| 2.1 | The Governing Equations | 3. |
| 2.2 | Boundary Conditions | 4. |
| 2.3 | Non-dimensional Form of Equations | 7. |
| 2.4 | The Dispersion Tensor | 8. |

Solution of the Equations 11.

- | | | |
|-----|-------------------------------------|-----|
| 3.1 | The Perturbation Expansion Approach | 11. |
| 3.2 | A Modified Iterative Scheme | 12. |
| 3.3 | Galerkin Finite Element Solution | 12. |
| 3.4 | The Unconfined Case | 20. |

Results 21.

- | | | |
|-----|--|-----|
| 4.1 | The Test Problem | 21. |
| 4.2 | Choice of Relaxation Factor | 25. |
| 4.3 | Effect of the Horizontal Flow Assumption | 25. |
| 4.4 | Flow Velocities | 30. |
| 4.5 | Effect of the Choice of a_L , a_T | 30. |
| 4.6 | The Unconfined Case | 34. |

Conclusions 41.

NOTATION: The following symbols have been used:

n	porosity (dimensionless)
D'_h	tensor coefficient of hydrodynamic dispersion (L^2T^{-1})
c	salt concentration (dimensionless)
\underline{q}	velocity vector (LT^{-1})
ρ	fluid density (ML^{-3})
K	hydraulic conductivity tensor (LT^{-1})
g	acceleration due to gravity (LT^{-2})
p'	pressure ($ML^{-1}T^{-2}$)
x', z'	coordinates in horizontal and downward vertical directions (L)
ρ_f	density of fresh water (ML^{-3})
ρ_s	maximum density of salt water present (ML^{-3})
α	constant (dimensionless)
\underline{n}	unit vector, outward normal to a boundary (dimensionless)
z'_0, z'_1, z'_2	elevations relative to origin (L)
h	thickness of aquifer (L)
\bar{p}	pressure due to head h of fresh water ($ML^{-1}T^{-2}$)
D_d	coefficient of molecular diffusion for salt in the aquifer (L^2T^{-1})
p, x, z, D	non-dimensionalized variables corresponding to p', x', z' and D'_h
z_0, z_1, z_2	non-dimensionalized elevations corresponding to z'_0, z'_1 and z'_2
D^*	non-dimensionalized mechanical dispersion tensor
a_L, a_T	longitudinal and transverse dispersivities (L)
\underline{v}	velocity vector (LT^{-1})
d_{50}	mean grain diameter (L)

c_0, c_1, c_2, \dots	}	coefficients in expansions of concentration
$\bar{c}_1, \bar{c}_2, \dots$		
c_1^*, c_2^*		

$p_0, p_1, p_2,$	}	coefficients in expansions of pressure
$\bar{p}_1, \bar{p}_2, \dots$		

ω relaxation factor

P tensor function

u, f, g, β scalar functions

\underline{r} vector function

Ω region

Γ_1, Γ_2 boundaries of Ω

w test function

u^h discrete approximation to u

ϕ_i basis functions (global numbering)

ϕ^i basis functions (local numbering)

H stiffness matrix

\underline{F} load vector

ξ, η local coordinates

$|J|$ Jacobian function

INTRODUCTION

In many arid and semi-arid regions, surface water is either scarce or unpredictable and groundwater often forms a major source of water supply. An understanding of the groundwater flow is required both in evaluating the size of the available resource and in developing the best strategy for its use. The problem is complicated by constraints on the water quality, depending on the particular use for which the water is required; this is of particular importance in coastal aquifers, where any increase in groundwater abstraction will cause saline water to move further inland, possibly endangering existing supplies. Since the amount of sodium chloride in sea water corresponds to approximately twenty times the safe limit for chloride in drinking water, it is clearly necessary to understand the interaction between the saline and the fresh water, and its effects on the flow in the aquifer.

This dissertation is concerned with investigating the conditions in a coastal aquifer; it will be assumed that the uniformity of the aquifer properties and flow conditions along the coast are such that the flow is essentially perpendicular to the coast. The problem can then be reduced to two dimensions, considering only the flows in a vertical plane at right angles to the coastline. The problem has been further simplified by considering here only the steady-state case, with no time dependence; it is proposed to extend the method to transient problems at a later stage.

Two distinct approaches are possible to the problem of modelling saline intrusion. The first considers the salt and fresh water as immiscible fluids separated by a sharp interface; this approximation can

greatly simplify the problem in many cases of practical interest, especially when certain assumptions relating to horizontal flow are also introduced (Bear¹). The fresh and salt water are in fact miscible fluids and a transition zone is formed at the interface as a result of hydrodynamic dispersion; the use of the abrupt interface approximation can only be justified where the width of the transition zone is relatively narrow.

The alternative approach which includes the effects of dispersion has developed from the work of Henry²; the problem is treated as one with continuous variation of salt concentration and density, resulting in an equation of motion and a solute transport equation which are coupled. This approach has been adopted for the work described in this dissertation.

EQUATIONS AND BOUNDARY CONDITIONS

2.1 The Governing Equations

The equations governing the steady state flow of water and the dispersion of salt in a porous medium can be written (Bear¹):

$$\nabla \cdot (nD'_h \nabla c) - \nabla \cdot (q c) = 0 \quad (2.1)$$

$$\nabla \cdot (\rho q) = 0 \quad (2.2)$$

$$q = \frac{-K}{\rho g} (\nabla p' - \rho g \nabla z') \quad (2.3)$$

$$\rho = \frac{\rho_s - \rho_f}{\rho_s - \rho_f} \rho_f \quad \text{or} \quad \rho = \rho_f (1 + \alpha c) \quad (2.4)$$

where $\alpha = \frac{\rho_s - \rho_f}{\rho_f}$, and the other symbols are as previously defined.

Substituting from equation (2.3) into (2.2):

$$\nabla \cdot \left(\frac{K}{g} \nabla p' - K \rho \nabla z' \right) = 0$$

and rearranging and making use of (2.4):

$$\nabla \cdot (K \nabla p') - g \rho_f \frac{\partial}{\partial z'} \left\{ K(1 + \alpha c) \right\} = 0 \quad (2.5)$$

If we assume K to be constant, then:

$$\nabla^2 p' = g \rho_f \alpha \frac{\partial c}{\partial z'} \quad (2.6)$$

Substituting from (2.4) into (2.1):

$$\nabla \cdot (nD'_h \nabla c) = \nabla \cdot \left(q \left(\frac{\rho_s - \rho_f}{\rho_s - \rho_f} \right) \right) = \frac{1}{\rho_s - \rho_f} \nabla \cdot (\rho q) - \frac{\rho_f}{\rho_s - \rho_f} \nabla \cdot q$$

The first term on the right hand side is zero by (2.2);
 substituting for \underline{q} from (2.3):

$$\nabla \cdot (nD_h \nabla c) = \frac{1}{\alpha g \rho_f} \nabla \cdot \left(\frac{K}{1+\alpha c} \nabla p \right) - \frac{1}{\alpha} \nabla \cdot (K \nabla z) \quad (2.7)$$

If we again assume K to be constant, then:

$$\nabla \cdot (nD_h \nabla c) = \frac{K}{\alpha g \rho_f} \nabla \cdot \left(\frac{1}{1+\alpha c} \nabla p \right) \quad (2.8)$$

2.2 Boundary Conditions

The equations (2.6) and (2.8) are to be solved simultaneously in some region, subject to boundary conditions on the concentration and the pressure. In the case of the coastal aquifer being modelled here, two cases need to be distinguished:

Case 1: The aquifer is confined (i.e. it is overlain by an impermeable layer). The flow domain being considered is OBCD, shown in Figure 1, where it is assumed that BC is sufficiently far inland for the water to be fresh and that the impermeable boundaries OB and DC are horizontal. Then taking the origin at O with coordinates x' horizontally and z' vertically downwards, the boundary conditions for the concentration are given by:

$$\left. \begin{array}{l} c = 0 \quad \text{on OD} \\ c = 0 \quad \text{on BC} \\ \frac{\partial c}{\partial z'} = 0 \quad \text{on OB and DC} \end{array} \right\} \quad (2.9)$$

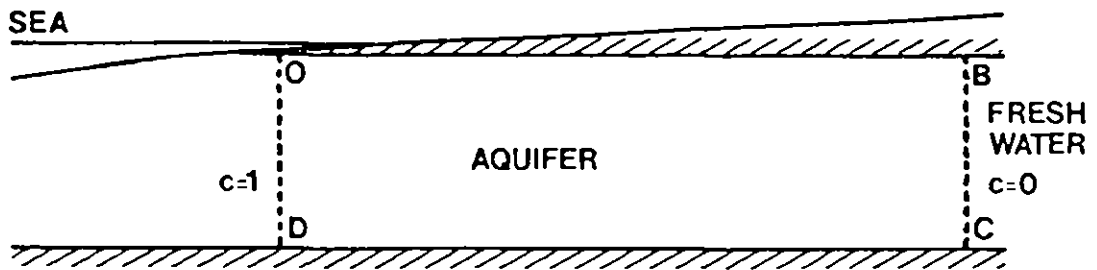


Figure 1 CROSS-SECTION THROUGH
 CONFINED COASTAL AQUIFER

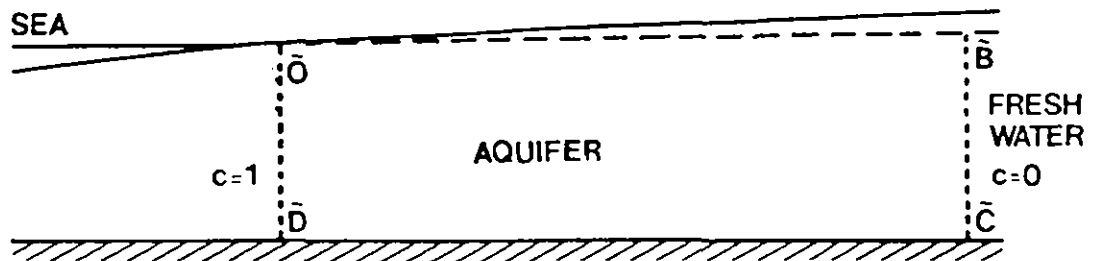


Figure 2 CROSS-SECTION THROUGH
 UNCONFINED COASTAL AQUIFER

The boundary conditions for the pressure are given by:

$$\begin{array}{rcl}
 & = \rho_s g(z'_0 - z') & \text{on OD} \\
 p' & = \rho_f g(z'_1 - z') & \text{on BC} \\
 \frac{\partial p'}{\partial z'} & = \rho_f(1 + \alpha c)g & \text{on OB and DC}
 \end{array} \quad \left. \vphantom{\begin{array}{rcl} & = \rho_s g(z'_0 - z') & \text{on OD} \\ p' & = \rho_f g(z'_1 - z') & \text{on BC} \\ \frac{\partial p'}{\partial z'} & = \rho_f(1 + \alpha c)g & \text{on OB and DC} \end{array}} \right\} \quad (2.10)$$

where z'_0 is the elevation of the sea surface and z'_1 is the head at B.

Case 2: The aquifer is unconfined (i.e. there is no confining layer overlying the aquifer and consequently the position of the top surface of the flow domain is unknown a priori). The flow now takes place in the region $\tilde{\text{OBCD}}$, shown in Figure 2; in this case the location of $\tilde{\text{B}}$ and the position of the boundary $\tilde{\text{OB}}$ are part of the required solution. Taking the origin at $\tilde{\text{O}}$, the boundary conditions for the concentration can now be written:

$$\begin{array}{rcl}
 & & \text{on } \tilde{\text{OD}} \\
 c & = 0 & \text{on } \tilde{\text{BC}} \\
 \frac{\partial c}{\partial z} & = 0 & \text{on } \tilde{\text{DC}} \\
 \frac{\partial c}{\partial n} & = 0 & \text{on } \tilde{\text{OB}}
 \end{array} \quad \left. \vphantom{\begin{array}{rcl} & & \text{on } \tilde{\text{OD}} \\ c & = 0 & \text{on } \tilde{\text{BC}} \\ \frac{\partial c}{\partial z} & = 0 & \text{on } \tilde{\text{DC}} \\ \frac{\partial c}{\partial n} & = 0 & \text{on } \tilde{\text{OB}} \end{array}} \right\} \quad (2.11)$$

where \underline{n} is the unit outward normal to the boundary $\tilde{\text{OB}}$.

The boundary conditions for the pressure are:

$$\begin{array}{rcl}
 p' & = -\rho_s g z' & \text{on } \tilde{\text{OD}} \\
 p' & = \rho_f g(z'_2 - z') & \text{on } \tilde{\text{BC}} \\
 \frac{\partial p'}{\partial z'} & = \rho_f(1 + \alpha c)g & \text{on } \tilde{\text{EC}} \\
 \frac{\partial p'}{\partial n} & = \rho_f(1 + \alpha c)g(-\underline{n} \cdot \underline{z}') \text{ and } p' = 0 & \text{on } \tilde{\text{OB}}
 \end{array} \quad \left. \vphantom{\begin{array}{rcl} p' & = -\rho_s g z' & \text{on } \tilde{\text{OD}} \\ p' & = \rho_f g(z'_2 - z') & \text{on } \tilde{\text{BC}} \\ \frac{\partial p'}{\partial z'} & = \rho_f(1 + \alpha c)g & \text{on } \tilde{\text{EC}} \\ \frac{\partial p'}{\partial n} & = \rho_f(1 + \alpha c)g(-\underline{n} \cdot \underline{z}') \text{ and } p' = 0 & \text{on } \tilde{\text{OB}} \end{array}} \right\} \quad (2.12)$$

where z'_2 is the elevation of \tilde{B} . The extra condition on $\tilde{O}\tilde{B}$ allows the position of the free surface to be determined.

2.3 Non-dimensional Form of Equations

The equations (2.6) and (2.8) can be written in non-dimensional form as follows. Let

$$\left. \begin{aligned} \rho' &= \bar{\rho} \rho \\ x' &= hx \\ z' &= hz \\ D'_h &= D_d D \end{aligned} \right\} \quad (2.13)$$

where h is the mean saturated thickness of the inland part of the aquifer under consideration, $\bar{\rho} = \rho_f gh$, D_d is the coefficient of molecular diffusion for salt in the aquifer and ρ , x , z and D are dimensionless.

From equation (2.6):

$$\frac{\bar{\rho}}{h^2} \nabla^2 p = g \rho_f \alpha \frac{\partial c}{h \partial z}$$

where now $\nabla = \left(\frac{\partial}{\partial x}, \frac{\partial}{\partial z} \right) = h \left(\frac{\partial}{\partial x'}, \frac{\partial}{\partial z'} \right)$

$$\nabla^2 p = \alpha \frac{\partial c}{\partial z} \quad (2.14)$$

From equation (2.8):

$$\frac{D_d}{h^2} \nabla (nD \nabla c) = \frac{K}{\alpha g \rho_f} \frac{\bar{\rho}}{h^2} \nabla \cdot \left(\frac{1}{1+\alpha c} \nabla p \right)$$

$$\frac{\alpha D_d}{hK} \nabla \cdot (nD \nabla c) = \nabla \cdot \left(\frac{1}{1+\alpha c} \nabla p \right) \quad (2.15)$$

The boundary conditions for the concentration (2.9) or (2.11) are clearly unaffected by the transformations represented by equations (2.13).

The boundary conditions for the pressure in the confined case, equations (2.10) become:

$$\left. \begin{aligned} \rho &= (1 + \alpha) (z_0 - z) && \text{on OD} \\ \rho &= (z_1 - z) && \text{on BC} \\ \frac{\partial \rho}{\partial z} &= (1 + \alpha c) && \text{on OB and DC.} \end{aligned} \right\} \quad (2.16)$$

In the case of the unconfined aquifer, corresponding to (2.12), we obtain:

$$\left. \begin{aligned} \rho &= -(1 + \alpha)z && \text{on } \tilde{OD} \\ \rho &= (z_2 - z) && \text{on } \tilde{BC} \\ \frac{\partial \rho}{\partial z} &= (1 + \alpha c) && \text{on } \tilde{DC} \\ \frac{\partial \rho}{\partial n} &= (1 + \alpha c) (-\underline{n} \cdot \underline{z}) \text{ and } p = 0 && \text{on } \tilde{OB} \end{aligned} \right\} \quad (2.17)$$

2.4 The Dispersion Tensor

Following Bear¹ the non-dimensionalized dispersion tensor D is of the form:

$$D = \frac{D_h}{D_d} \{ I + D^* \} \quad (2.18)$$

where the non-dimensionalized mechanical dispersion tensor D^* can be

written as:

$$\left(D_{ij}^* \right) = \frac{1}{D_d} \begin{pmatrix} (a_L V_x^2 + a_T V_z^2)/|V| & (a_L - a_T) V_x V_z / |V| \\ (a_L - a_T) V_x V_z / |V| & (a_T V_x^2 + a_L V_z^2)/|V| \end{pmatrix} \quad (2.19)$$

where a_L , a_T are the longitudinal and transverse dispersivities of the medium (assumed isotropic) and

$$\underline{V} = \underline{q}/n = \frac{-K}{n(1+\alpha c)} \left[\underline{\nabla} p - (1+\alpha c) \underline{\nabla} z \right] \quad (2.20)$$

Equation (2.19) can be simplified by making the assumption that the flow is essentially horizontal with $V_x \gg V_z$ (Wikramaratna and Wood⁵); D^* is then given approximately by the diagonal matrix

$$\left(D_{ij}^* \right) \approx \frac{|V|}{D_d} \begin{pmatrix} a_L & 0 \\ 0 & a_T \end{pmatrix} \quad (2.21)$$

Various different assumptions have been made about the values taken for the dispersivities a_L and a_T . Bear¹ suggests that they should be obtained for each site from the solution of an inverse problem. Nishi, Bruch and Lewis³, in considering the seepage of pollutants from a triangular ditch, take $a_L = 1.8 d_{50}$ where d_{50} is the mean grain diameter. On the other hand, Frind⁴, discussing a coastal aquifer-aquitard system, takes the dispersivities as proportional to the depth of the aquifer; he takes $a_L = h/6$, $a_T = a_L/10$.

For the work described here, the dispersivities have been assumed to be related to the depth of the aquifer; solutions have been obtained

with a series of different values of a_L and a_T to allow comparison of the results. The full form of the dispersion tensor (2.19) has been used in obtaining solutions, allowing an evaluation of the effects of the horizontal flow approximation, equation (2.21), used by Wikramaratna and Wood⁵.

SOLUTION OF THE EQUATIONS

3.1 The Perturbation Expansion Approach

Wikramaratna and Wood⁵ take α as a convenient 'small' parameter to use as the basis for perturbation expansions for equations (2.14) and (2.15), putting

$$c = c_0 + \alpha c_1 + \alpha^2 c_2 + \dots \quad (3.1)$$

$$p = p_0 + \alpha p_1 + \alpha^2 p_2 + \dots \quad (3.2)$$

Orthodox perturbation methods (Van Dyke⁶) would solve for p_0 , c_0 , p_1 , c_1 , etc. separately with boundary conditions from the terms of matching order, but Wikramaratna and Wood found it more convenient in obtaining numerical solutions to solve for p_0 , c_0 , $\bar{p}_1 = p_0 + \alpha p_1$, $\bar{c}_1 = c_0 + \alpha c_1$, etc., using the full boundary conditions each time. This leads to the numerical scheme

$$\nabla^2 p_0 = 0 \quad (3.3)$$

$$\frac{D_d}{hK} \nabla \cdot (nD(V_0) \nabla c_0) - \nabla c_0 \cdot \nabla p_0 = 0 \quad (3.4)$$

$$\nabla^2 \bar{p}_n = \alpha \frac{\partial \bar{c}_{n-1}}{\partial z} \quad (3.5)$$

$$\begin{aligned} \frac{D_d}{hK} \nabla \cdot (nD(V_n) \nabla \bar{c}_n) + \frac{1}{(1+\alpha \bar{c}_{n-1})^2} \nabla \bar{c}_n \cdot \nabla \bar{p}_n \\ - \frac{1}{(1+\alpha \bar{c}_{n-1})} \frac{\partial \bar{c}_n}{\partial z} = 0 \end{aligned} \quad (3.6)$$

where the dispersion tensor is calculated at each stage from equations (2.18) and (2.19) or (2.21) and with the velocities given by equation (2.20) using the most recent estimates of the pressure and concentration.

3.2 A Modified Iterative Scheme

In practice it was found that the iterative scheme given by equations (3.3) - (3.6) failed to converge when realistic values were taken for the molecular diffusion D_d . In order to overcome these difficulties, a modified iterative scheme has been developed. Equations (3.3), (3.4) and (3.5) remain unaltered, while equation (3.6) is replaced by a two-stage calculation

$$\frac{D_d}{hK} \underline{\nabla} \cdot (nD(\underline{v}_n) \underline{\nabla} c_n^*) + \frac{1}{(1+\alpha \bar{c}_{n-1})^2} \underline{\nabla} c_n^* \cdot \underline{\nabla} \bar{p}_n - \frac{1}{(1+\alpha \bar{c}_{n-1})} \frac{\partial c_n^*}{\partial z} = 0 \quad (3.7)$$

$$\bar{c}_n = \omega c_n^* + (1-\omega) \bar{c}_{n-1} \quad (3.8)$$

Clearly $\omega = 1$ leads to the scheme obtained from the perturbation expansion approach. A choice of $\omega = 0.5$ was found to give a very significant improvement in the convergence of the scheme over the whole range of parameter values used; this value of ω has been used in obtaining most of the results presented in section 4.

3.3 Galerkin Finite Element Solution

The equations for the pressure and the concentration have been solved at each iteration using the Galerkin finite element method, with isoparametric quadrilateral elements and bilinear basis functions (Strang and Fix⁷; Zienkiewicz⁸).

Consider the second order partial differential equation:

$$-\underline{\nabla} \cdot (P \underline{\nabla} u) + \underline{r} \cdot \underline{\nabla} u = f \quad (3.9)$$

where the symmetric tensor P , the vector \underline{r} and the scalar f are known functions of position. The equation (3.9) holds in some region Ω , with boundary conditions:

$$\left. \begin{array}{ll} u = g & \text{on } \Gamma_1 \\ (P\underline{\nabla}u) \cdot \underline{n} = \beta & \text{on } \Gamma_2 \end{array} \right\} \quad (3.10)$$

where $\Gamma_1 + \Gamma_2$ is the boundary of Ω and \underline{n} is the unit outward normal from Ω .

It is clear that each stage of the iteration both the pressure equation (3.5) with boundary conditions (2.16) and the concentration equation (3.6) or (3.7) with boundary conditions (2.9) are of this form, and it is sufficient simply to consider the solution of the problem defined by equations (3.9) and (3.10).

A weak form of the differential equation (3.9) is obtained by forming an inner product with a test function w :

$$\iint_{\Omega} \left[-\underline{\nabla} \cdot (P\underline{\nabla}u) + \underline{r} \cdot \underline{\nabla}u \right] w \, d\Omega = \iint_{\Omega} f w \, d\Omega \quad (3.11)$$

Hence, integrating by parts

$$\begin{aligned} & - \int_{\Gamma_1} w (P\underline{\nabla}u) \cdot \underline{n} \, ds - \int_{\Gamma_2} w (P\underline{\nabla}u) \cdot \underline{n} \, ds \\ & + \iint_{\Omega} \left[(P\underline{\nabla}u) \cdot \underline{\nabla}w + (\underline{r} \cdot \underline{\nabla}u) w \right] d\Omega = \iint_{\Omega} f w \, d\Omega \end{aligned} \quad (3.12)$$

Using the boundary conditions on Γ_2

$$\iint_{\Omega} \left((P \underline{\nabla} u) \cdot \underline{\nabla} w + (\underline{r} \cdot \underline{\nabla} u) w \right) d\Omega = \iint_{\Omega} f w d\Omega + \int_{\Gamma_2} \beta w ds \quad (3.13)$$

with the understanding that $u = g$ on Γ_1 .

The function u is approximated in (3.13) by:

$$u \approx u^h = \sum_{i=1}^n u_i \phi_i \quad (3.14)$$

where the ϕ_i are basis functions, and it is required that $u^h = g$ at the nodes on Γ_1 ; putting $w = \phi_j$ in turn then leads to a set of n simultaneous equations of the form:

$$\begin{aligned} \sum_{i=1}^n u_i \iint_{\Omega} \left[(P \underline{\nabla} \phi_i) \cdot \underline{\nabla} \phi_j + (\underline{r} \cdot \underline{\nabla} \phi_i) \phi_j \right] d\Omega \\ = \iint_{\Omega} f \phi_j d\Omega + \int_{\Gamma_2} \beta \phi_j ds \quad i = 1, \dots, n \end{aligned} \quad (3.15)$$

These equations can be written in matrix form as:

$$H \underline{u} = \underline{F} + \underline{g} \quad (3.16)$$

where H is the 'stiffness' matrix and \underline{F} is the load vector.

In the finite element method the ϕ_i are 'local' - the region Ω is divided into elements whose vertices are called nodes, and the ϕ_i are such that:

$$\phi_i = \begin{cases} 1 & \text{at node } i \\ 0 & \text{at every other node} \end{cases} \quad (3.17)$$

The u_i are called the nodal coordinates. Suppose that the point Q is at node i ; then $\phi_i(Q) = 1$ and $\phi_j(Q) = 0$ for any $j \neq i$ and

$$u^h(Q) = u_i \quad (3.18)$$

Suppose that the region Ω has been divided in a suitable fashion into N quadrilateral elements, and suppose that the sub-region Ω_ℓ represents the ℓ -th element. Entries in the 'stiffness' matrix are of the form:

$$\begin{aligned} H_{ij} &= \iint_{\Omega} \left(P_{11} \frac{\partial \phi_i}{\partial x} \frac{\partial \phi_j}{\partial x} + P_{12} \left(\frac{\partial \phi_i}{\partial x} \frac{\partial \phi_j}{\partial z} + \frac{\partial \phi_i}{\partial z} \frac{\partial \phi_j}{\partial x} \right) + P_{22} \frac{\partial \phi_i}{\partial z} \frac{\partial \phi_j}{\partial z} \right. \\ &\quad \left. + r_1 \frac{\partial \phi_i}{\partial x} \phi_j + r_2 \frac{\partial \phi_i}{\partial z} \phi_j \right) dx dz \\ &= \sum_{\ell=1}^n \iint_{\Omega_\ell} \left(P_{11} \frac{\partial \phi_i}{\partial x} \frac{\partial \phi_j}{\partial x} + P_{12} \left(\frac{\partial \phi_i}{\partial x} \frac{\partial \phi_j}{\partial z} + \frac{\partial \phi_i}{\partial z} \frac{\partial \phi_j}{\partial x} \right) + P_{22} \frac{\partial \phi_i}{\partial z} \frac{\partial \phi_j}{\partial z} \right. \\ &\quad \left. + r_1 \frac{\partial \phi_i}{\partial x} \phi_j + r_2 \frac{\partial \phi_i}{\partial z} \phi_j \right) dx dz \\ &= \sum_{\ell=1}^n I_{ij\ell} \end{aligned} \quad (3.19)$$

For each element, a transformation is made to local coordinates (ξ, η) on a canonical square using the isoparametric transformation:

$$\left. \begin{aligned} x &= \sum_{j=1}^n x_j \phi_j(\xi, \eta) \\ z &= \sum_{j=1}^n z_j \phi_j(\xi, \eta) \end{aligned} \right\} \quad (3.20)$$

Hence

$$\left. \begin{aligned} \frac{\partial \phi_i}{\partial x} &= \frac{\partial \phi_i}{\partial \xi} \frac{\partial \xi}{\partial x} + \frac{\partial \phi_i}{\partial \eta} \frac{\partial \eta}{\partial x} \\ \frac{\partial \phi_i}{\partial z} &= \frac{\partial \phi_i}{\partial \xi} \frac{\partial \xi}{\partial z} + \frac{\partial \phi_i}{\partial \eta} \frac{\partial \eta}{\partial z} \end{aligned} \right\} (3.21)$$

Now

$$\left. \begin{aligned} dx &= \frac{\partial x}{\partial \xi} d\xi + \frac{\partial x}{\partial \eta} d\eta \\ dz &= \frac{\partial z}{\partial \xi} d\xi + \frac{\partial z}{\partial \eta} d\eta \end{aligned} \right\} (3.22)$$

which leads to

$$\left. \begin{aligned} d\xi &= \frac{1}{|J|} \left(\frac{\partial z}{\partial \eta} dx - \frac{\partial x}{\partial \eta} dz \right) \\ d\eta &= \frac{1}{|J|} \left(-\frac{\partial z}{\partial \xi} dx + \frac{\partial x}{\partial \xi} dz \right) \end{aligned} \right\} (3.23)$$

where

$$|J| = \frac{\partial x}{\partial \xi} \frac{\partial z}{\partial \eta} - \frac{\partial x}{\partial \eta} \frac{\partial z}{\partial \xi} \quad (3.24)$$

Also

$$\left. \begin{aligned} d\xi &= \frac{\partial \xi}{\partial x} dx + \frac{\partial \xi}{\partial z} dz \\ d\eta &= \frac{\partial \eta}{\partial x} dx + \frac{\partial \eta}{\partial z} dz \end{aligned} \right\} (3.25)$$

and comparison of terms in equations (3.23) and (3.25) give:

$$\begin{aligned}
\frac{\partial \xi}{\partial x} &= \frac{1}{|J|} \frac{\partial z}{\partial \eta} = \frac{1}{|J|} \sum_{j=1}^n z_j \frac{\partial \phi_j}{\partial \eta} \\
\frac{\partial \xi}{\partial z} &= -\frac{1}{|J|} \frac{\partial x}{\partial \eta} = -\frac{1}{|J|} \sum_{j=1}^n x_j \frac{\partial \phi_j}{\partial \eta} \\
\frac{\partial \eta}{\partial x} &= -\frac{1}{|J|} \frac{\partial z}{\partial \xi} = -\frac{1}{|J|} \sum_{j=1}^n z_j \frac{\partial \phi_j}{\partial \xi} \\
\frac{\partial \eta}{\partial z} &= \frac{1}{|J|} \frac{\partial x}{\partial \xi} = \frac{1}{|J|} \sum_{j=1}^n x_j \frac{\partial \phi_j}{\partial \xi}
\end{aligned}
\tag{3.26}$$

where use has been made of equations (3.20) in obtaining the expressions on the right.

Suppose that we adopt a local numbering system for the nodes, as shown in figure 3, and represent the local numbering by superscripts. Then for the bilinear elements:

$$\begin{aligned}
\phi^1 &= \frac{1}{4}(1+\xi)(1+\eta) \\
\phi^2 &= \frac{1}{4}(1-\xi)(1+\eta) \\
\phi^3 &= \frac{1}{4}(1-\xi)(1-\eta) \\
\phi^4 &= \frac{1}{4}(1+\xi)(1-\eta)
\end{aligned}
\tag{3.27}$$

and all the other basis functions are identically zero within the element. Hence:

$$\begin{aligned}
\frac{\partial \phi^1}{\partial \xi} &= \frac{1}{4}(1+\eta) & \frac{\partial \phi^1}{\partial \eta} &= \frac{1}{4}(1+\xi) \\
\frac{\partial \phi^2}{\partial \xi} &= -\frac{1}{4}(1+\eta) & \frac{\partial \phi^2}{\partial \eta} &= \frac{1}{4}(1-\xi) \\
\frac{\partial \phi^3}{\partial \xi} &= -\frac{1}{4}(1-\eta) & \frac{\partial \phi^3}{\partial \eta} &= -\frac{1}{4}(1-\xi) \\
\frac{\partial \phi^4}{\partial \xi} &= \frac{1}{4}(1-\eta) & \frac{\partial \phi^4}{\partial \eta} &= -\frac{1}{4}(1+\xi)
\end{aligned}
\tag{3.28}$$

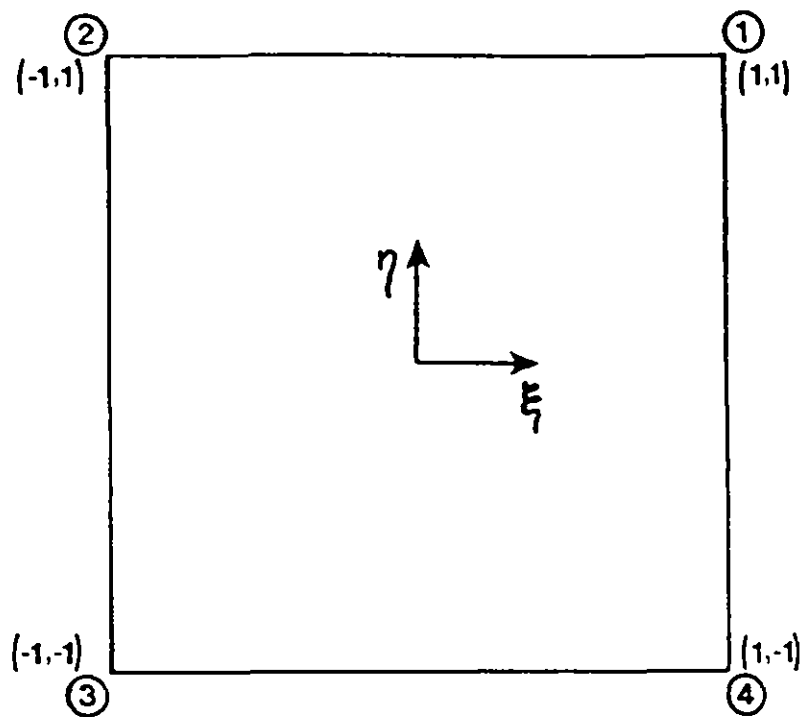


Figure 3 LOCAL COORDINATES ON
A CANONICAL SQUARE

Clearly in evaluating the terms $I_{ij\ell}$ in equation (3.19) a non-zero value will only be obtained for $I_{ij\ell}$ if nodes i and j (in the global numbering system) both fall on the boundary of element ℓ . Hence there will be non-zero contributions to the summation from at most two of the elements. The non-zero $I_{ij\ell}$ can be evaluated by substituting for $\frac{\partial\phi_i}{\partial x}$, $\frac{\partial\phi_i}{\partial z}$, $\frac{\partial\phi_j}{\partial x}$, $\frac{\partial\phi_j}{\partial z}$ from equations (3.21) and then making use of equations (3.26), (3.27) and (3.28) and the relationship:

$$dx dy = |J| d\xi d\eta \quad (3.29)$$

to obtain an expression for $I_{ij\ell}$ in which the integrand is given in terms of P_{11} , P_{12} , P_{22} and simple functions of ξ , η and the integration is to be performed over the square $-1 < \xi < 1$, $-1 < \eta < 1$. The integral can be evaluated numerically using four-point Gauss-Legendre quadrature with the sampling points given by $\xi = \pm 1/\sqrt{3}$, $\eta = \pm 1/\sqrt{3}$.

The elements F_j of the load vector can be similarly evaluated using the equation

$$F_j = \iint_{\Omega} f\phi_j dx dy = \sum_{\ell=1}^N \iint_{\Omega_{\ell}} f\phi_j dx dy \quad (3.30)$$

and in this case there will only be a non-zero contribution to the summation if node j is on the boundary of element ℓ .

After assembly, the matrix equations (3.16) have been solved using NAG subroutines F018MF and F04AVF. The subroutine F018MF decomposes the real banded matrix H into triangular sub-matrices using Gaussian elimination with pivoting, making use of the band structure

to reduce the storage requirements. The subroutine F04AVF uses this decomposition to obtain the solution.

3.4 The Unconfined Case

The iterative scheme has been further modified to deal with the case of an unconfined aquifer. Initial estimates of pressure and concentration are obtained exactly as for the confined aquifer using equations (3.3) and (3.4) and ignoring the extra condition $p = 0$ on \tilde{OB} (equation 2.17). At each stage of the iteration the positions of the nodes lying on the free surface are adjusted in a vertical direction, after which new estimates of the pressure and concentration are obtained using equations (3.5), (3.7) and (3.8). Suppose that node k is on the free surface and at the n -th iteration it had z -coordinate $z_n(k)$ with corresponding pressure and concentration solutions $\bar{p}_n(k)$ and $\bar{c}_n(k)$. Then the new z -coordinate is given by:

$$z_{n+1}(k) = z_n(k) - \frac{\bar{p}_n(k)}{1 + \alpha \bar{c}_n(k)} \quad (3.31)$$

The use of this equation is motivated by the fact that with zero pressure at $z_{n+1}(k)$, a constant concentration $\bar{c}_n(k)$ and a hydrostatic pressure distribution, the pressure at $z_n(k)$ would be equal to $\bar{p}_n(k)$.

RESULTS

4.1 The Test Problem

The methods discussed above have been tested on an example based on the Mogadishu coastal plain in Somalia. The Mogadishu aquifer is a thick semi-consolidated sand aquifer which passes laterally into arenaceous limestone towards the coast. The following model dimensions and parameter values based on the Mogadishu aquifer have been used for the test problem.

Permeability	$K = 10^{-4} \text{ ms}^{-1}$
Aquifer depth	$h = 100 \text{ m}$
Porosity	$n = 0.4$
	$\alpha = 0.02$

An aquifer length of 500 m was found to be sufficient: further increases in the modelled aquifer length were found to have no significant effect on the solutions obtained and this value was used in all the model runs described below.

For the confined case, values for z'_0 and z'_1 of 0.0 and 2.2 m were used, while for the unconfined case, the value of z'_2 was taken as 2.2 m.

Table I summarises the other parameter values for the runs discussed below. Figure 4 illustrates the finite element mesh used for the test problem.

The coefficient of molecular diffusion for sodium chloride in solution is given by Weast, Selby and Hodgman⁹ as $1.5 \times 10^{-9} \text{ m}^2 \text{ s}^{-1}$.

Run Number	D_d	a_L/h	a_T/h	ω	Mechanical Dispersion	Top Boundary Condition
8A	10^{-5}	.25	.05	1.0	Horiz. Flow Assumption	Confined
8B	10^{-6}	.25	.05	1.0	Horiz. Flow Assumption	Confined
12A	10^{-5}	.25	.05	0.5	Horiz. Flow Assumption	Confined
12B	10^{-6}	.25	.05	0.5	Horiz. Flow Assumption	Confined
15E	10^{-9}	.10	.01	0.5	Horiz. Flow Assumption	Confined
25E	10^{-9}	.10	.01	0.5	Full Disp. Tensor	Confined
26E	10^{-9}	.05	.005	0.5	Full Disp. Tensor	Confined
27E	10^{-9}	.025	.0025	0.5	Full Disp. Tensor	Confined
35E	10^{-9}	.10	.01	0.5	Full Disp. Tensor	Unconfined

Table I

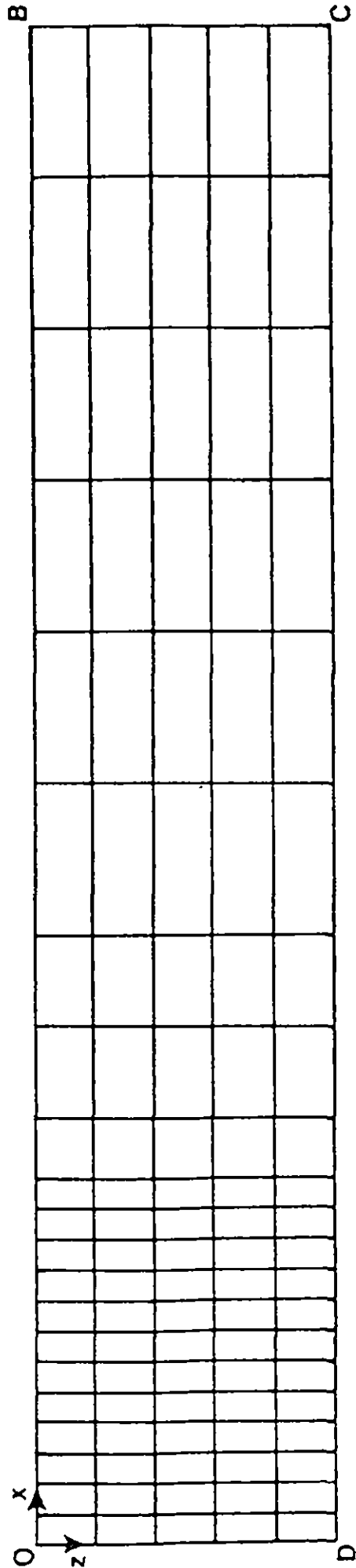


Figure 4 FINITE ELEMENT MESH FOR TEST PROBLEM
[NON-DIMENSIONAL DEPTH = 1.0, LENGTH = 5.0]

Following Bear, the effect of the porous medium is to reduce the molecular diffusion coefficient by a factor m , where $\frac{1}{3} < m < \frac{2}{3}$. Taking $m = \frac{2}{3}$, this gives a value of $D_d = 10^{-9} \text{ m}^2 \text{ s}^{-1}$ for the coefficient of molecular diffusion in the aquifer. In some cases it proved impossible to obtain convergence with such a small value of D_d , and it was necessary to use larger values for some of the runs in order to compare the different schemes. The run numbers used to identify the various runs consist of a two-digit number followed by a letter. The letter identifies the value used for D_d :

$$D_d = 10^{-5}$$

$$D_d = 10^{-6}$$

$$D_d = 10^{-9}$$

Thus, for example, runs 12A, 12B and 12E all have identical parameters except for the value of D_d .

The criterion for convergence is based on the maximum change in concentration:

$$\max |c_n^* - \bar{c}_{n-1}| < 0.1 \quad (4.1)$$

where c_n^* and \bar{c}_{n-1} are as used in equation (3.7) and where the maximum is taken over the nodal values. This measure of convergence has been adopted, rather than the alternative of looking at $\max |\bar{c}_n - \bar{c}_{n-1}|$, since it is independent of the choice of relaxation factor ω .

4.2 Choice of Relaxation Factor

Initial runs were made using the iterative scheme described in section 3.2 with a value of $\omega = 1.0$ (that is, following the scheme used by Wikramaratna and Wood⁵). In order to obtain convergence with this scheme, it was necessary to use values of D_d as large as 10^{-6} or 10^{-5} . Figure 5 shows the $c = 0.5$ isochlors for successive iterations for run 8B; it will be observed that the solutions for the 'odd' iterations (C3, C5, C7) and those for the 'even' iterations (C4, C6, C8) are in each case closely grouped but the solution oscillates back and forth between these two distinct groups.

Subsequently a value of $\omega = 0.5$ was tried, and was found to give much more satisfactory results. Figure 6 shows the successive $c = 0.5$ isochlors for run 12B; the only difference between runs 8B and 12B was in the value taken for ω . Figure 7 illustrates the improved convergence obtained with $\omega = 0.5$, showing the maximum nodal change in the concentration solution at each iteration for the two runs. Figure 8 shows the corresponding convergence rates for runs 8A and 12A; although in this case both schemes converged, it is clear from the diagram that the convergence is improved by taking $\omega = 0.5$.

The choice of $\omega = 0.5$ resulted in satisfactory convergence over a wide range of parameter values, and this value of ω has been used for all the other runs discussed below.

4.3 Effect of the Horizontal Flow Approximation

Wikramaratna and Wood⁵ assumed that the flow was essentially horizontal allowing the use of the simplified form of the dispersion tensor given by equation (2.21). The program has been modified to

C:0.5 CONTOURS FOR SUCCESSIVE ITERATIONS

RUN 8B $D_d=10^{-6}$ $a_L/h=0.25$ $a_T/h=0.05$ $\omega=1.0$

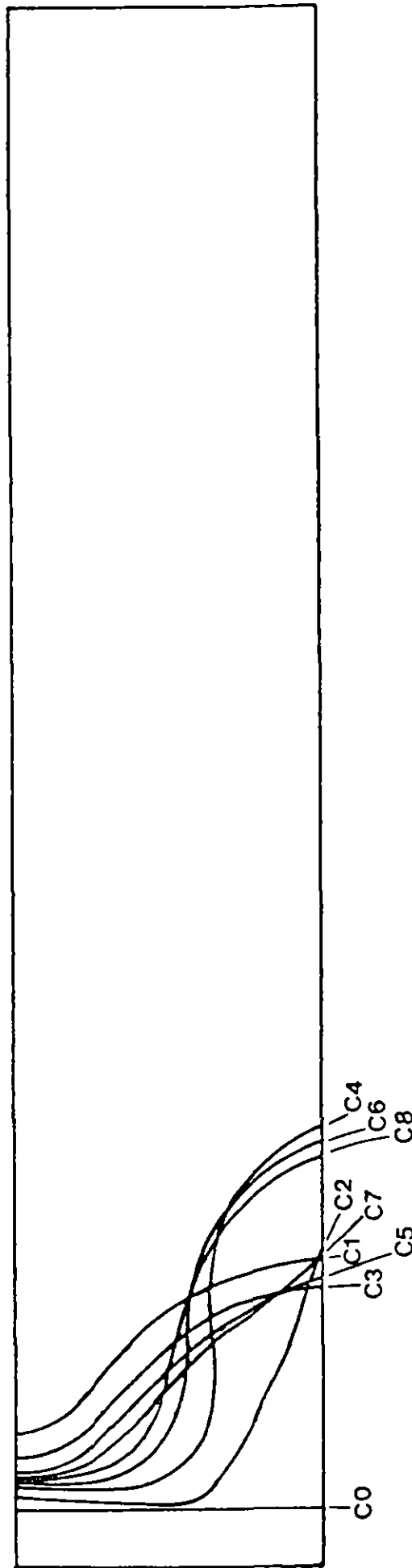


Figure 5

C=0.5 CONTOURS FOR SUCCESSIVE ITERATIONS

RUN 12B $D_d=10^{-6}$ $a_L/h=0.25$ $a_T/h=0.05$ $\omega=0.5$

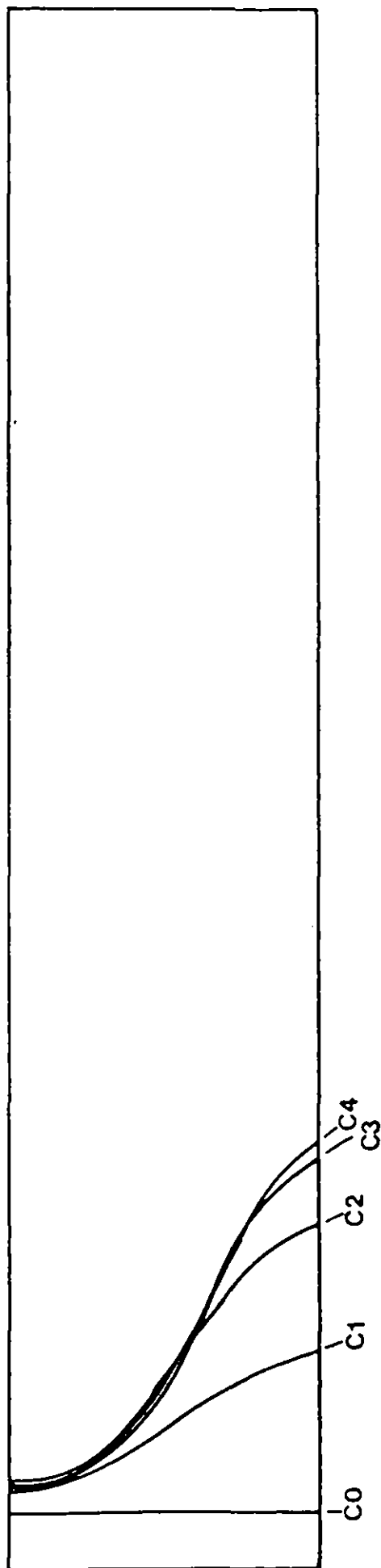


Figure 6

CONVERGENCE OF ITERATION

$D_0=10^{-5}$ $a_L/h=0.25$ $a_T/h=0.05$

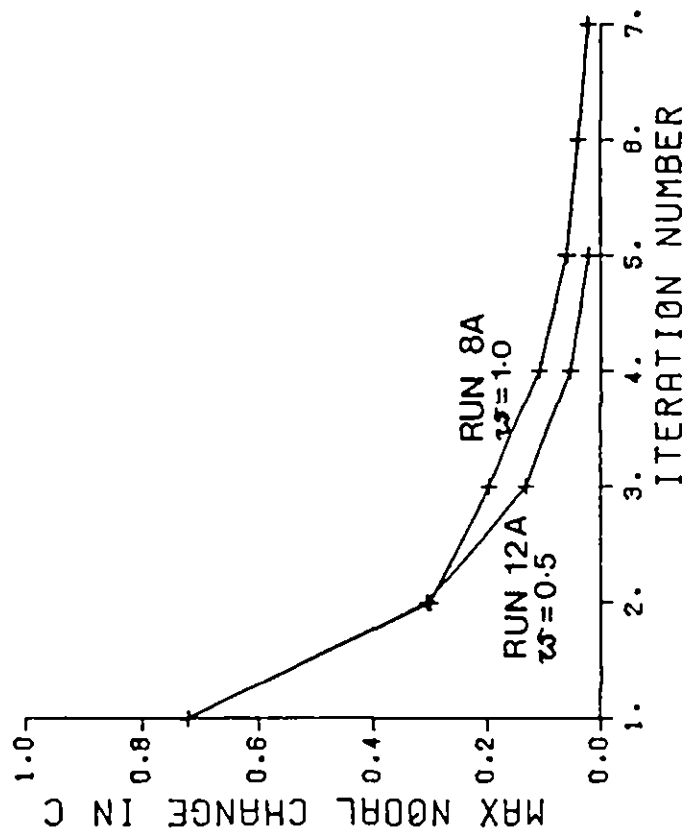


Figure 7

CONVERGENCE OF ITERATION

$D_H=10^{-6}$ $a_L/h=0.25$ $a_T/h=0.05$

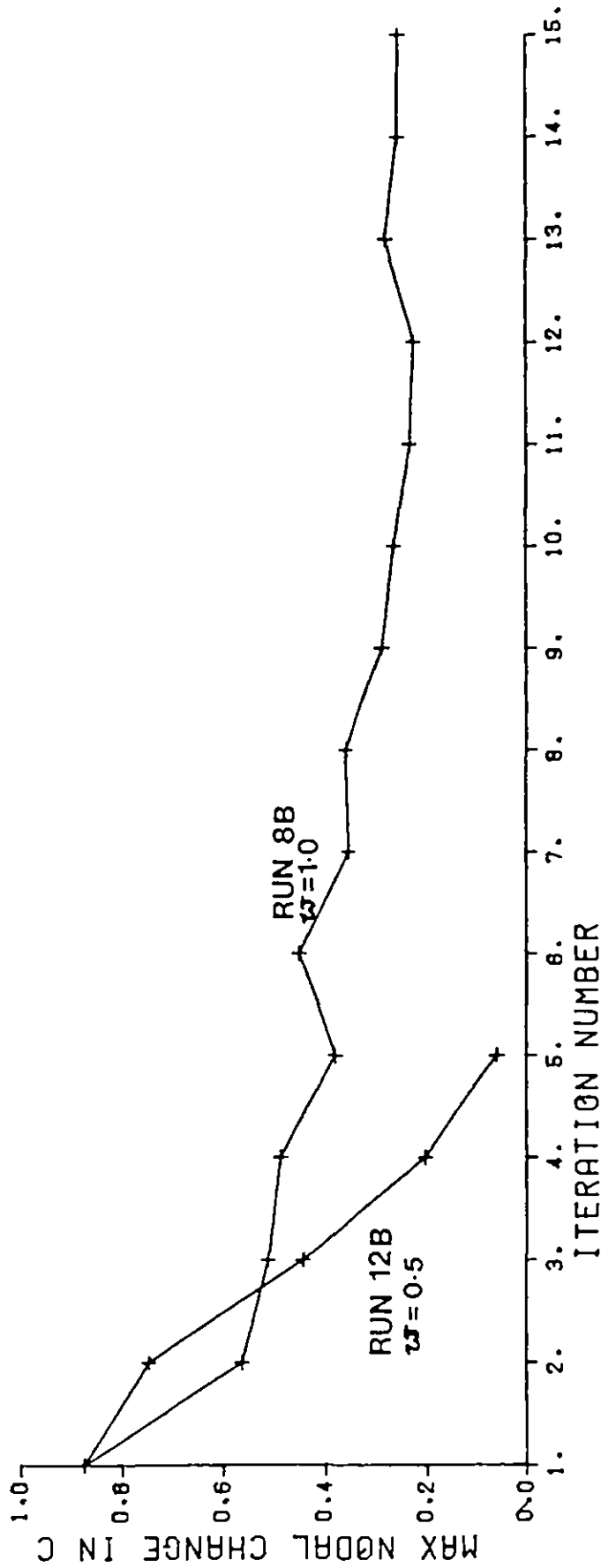


Figure 8

make use of the full dispersion tensor, equations (2.19), allowing an assessment of the effects of the approximation. Figure 9 compares the positions of the $c = 0.25$, 0.5 and 0.75 isochlors for run 15E which uses the horizontal flow approximation and run 25E which uses the full form of the dispersion tensor. The main effect of using the horizontal flow approximation is to bring the 'toe' of the saline wedge further inland than with the full dispersion tensor, but it has relatively little effect on the spread of the isochlors. Figure 10 shows the convergence for the two runs; clearly the horizontal flow approximation results in a small reduction in the number of iterations required.

4.4 Flow Velocities

Figure 11 shows the velocity vectors obtained for run 25E, using equation (2.20) to calculate the velocities for the converged pressure solution, together with the $c = 0.25$, 0.5 and 0.75 isochlors. The circulatory motion of the saline water, flowing in at the bottom of the aquifer and flowing out together with the fresh water in the upper part of the aquifer has been described by Henry and has also been observed in field measurements². This circulation results in the increasing flow velocities at the top of the aquifer as the coast is approached, since the water passing through the aquifer is flowing out through a continually decreasing cross section of the aquifer.

4.5 Effect of the Choice of a_L , a_T

Runs 25E, 26E and 27E illustrate the effect of reducing the values of a_L and a_T while keeping a_L/a_T constant. Figure 12, which compares the convergence for the three runs, shows that a reduction in a_L and a_T leads to a slower rate of convergence. The concentration

CONVERGED CONCENTRATION SOLUTIONS $D_D=10^{-9}$ $a_U/h=0.1$ $a_T/h=0.01$

RUN 15E [C6] - - - - - HORIZONTAL FLOW APPROXIMATION

RUN 25E [C7] ——— FULL DISPERSION TENSOR

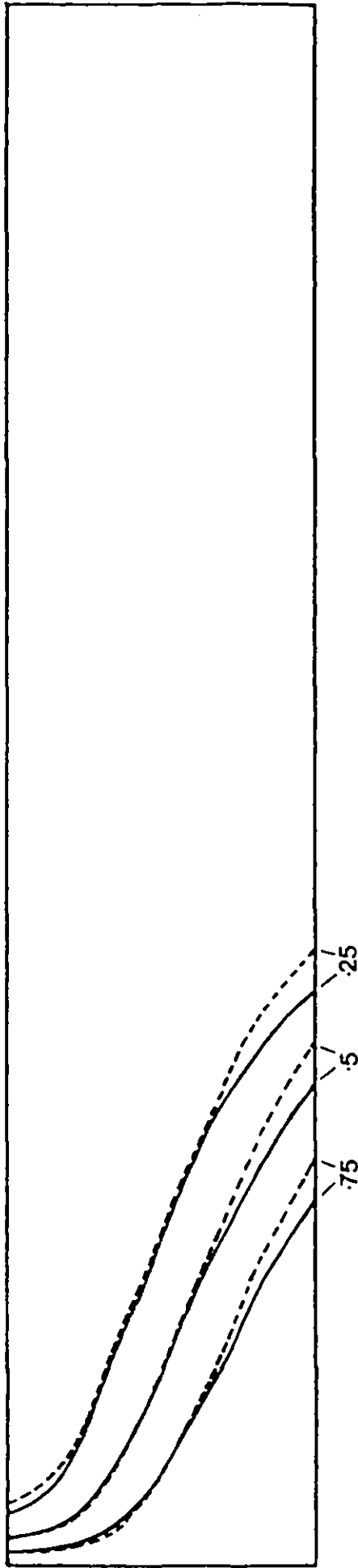


Figure 9

CONVERGENCE OF ITERATION

$D_d=10^{-9}$ $a_L/h=0.1$ $a_T/h=0.01$

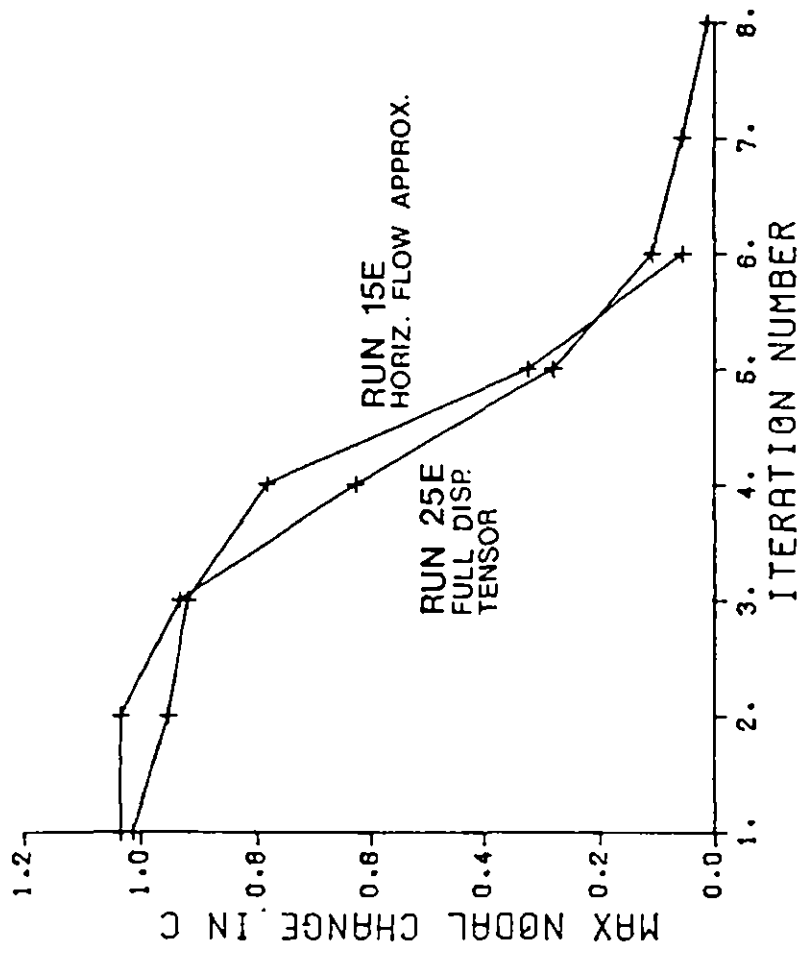


Figure 10

RUN 25E

FULL DISPERSION TENSOR

$D_f = 10^{-9}$ $a_L/h = 0.1$ $a_T/h = 0.01$

SCALE:

\rightarrow 0.000000250

\rightarrow 0.000000125

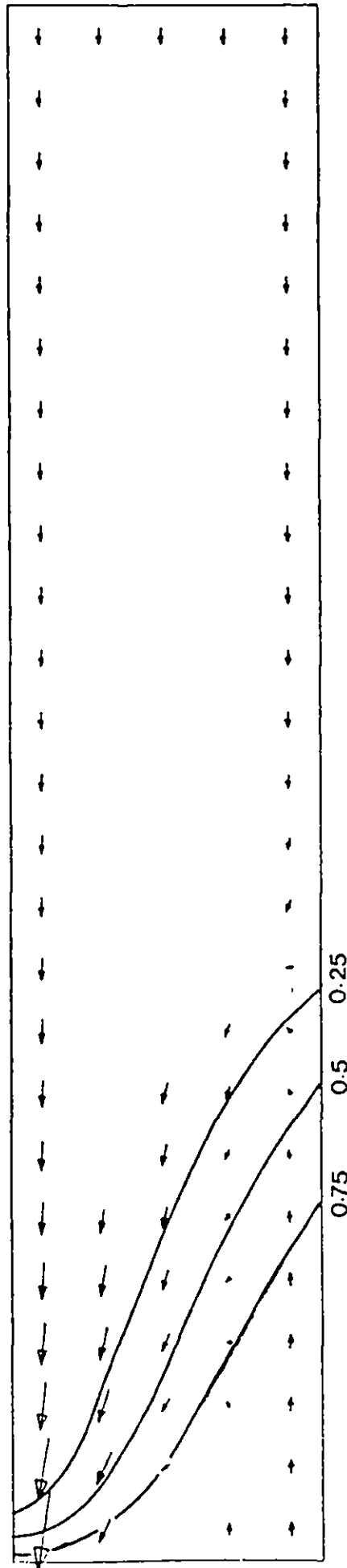


Figure 11 VELOCITY VECTORS AND ISOCHLORS FOR CONVERGED SOLUTION

varies most rapidly in the region of the origin along the x-direction and it is to be expected that any oscillations in the converged solutions will manifest themselves in this area; figures 13, 14 and 15 show the converged concentration solutions along $z = 0$ for $0 \leq x \leq 0.5$ for the three runs. For run 25E, (figure 13), with a value of $a_L/d = 0.1$, the concentration solution reduces smoothly from $c = 1$ at $x = 0$ to $c = 0$. For run 26E (figure 14), $a_L/d = 0.05$ and the solution is effectively zero for $x > 0.1$; although there is some oscillation of the solution, it is so slight as to be almost negligible. For run 27E (figure 15), $a_L/d = 0.025$ and the solution has large oscillations; it seems that in the region of $x = 0$ the mesh is too coarse to cope with the changes in concentration occurring there.

Figure 16 compares the concentration solutions for runs 25E and 26E; the main effect of reducing a_L/d is to bring the isochlors much closer together in the vicinity of $x = 0, z = 0$; the isochlors in the main body of the aquifer are also slightly closer together, but the effect is much less marked here.

4.6 The Unconfined Case

Run 35E represents the unconfined case corresponding to run 25E; the parameter values for the two runs are identical, and the only difference is in the treatment of the top boundary condition. Figure 17 compares the convergence of the salt concentration in the two cases; a slight increase in the number of iterations required in the unconfined case is the result of the changes in position of the free surface between iterations. Figure 18 shows the maximum change in free surface elevation at each iteration; it is clear from comparison with figure 17

that the changes in free surface position reduce more rapidly than the changes in concentration, so that the convergence of the whole iteration is in fact governed by the convergence of the concentration solution. The positions of the $c = 0.25$, 0.5 and 0.75 isochlors for run 35E are indistinguishable to plotting accuracy from those obtained with run 25E.

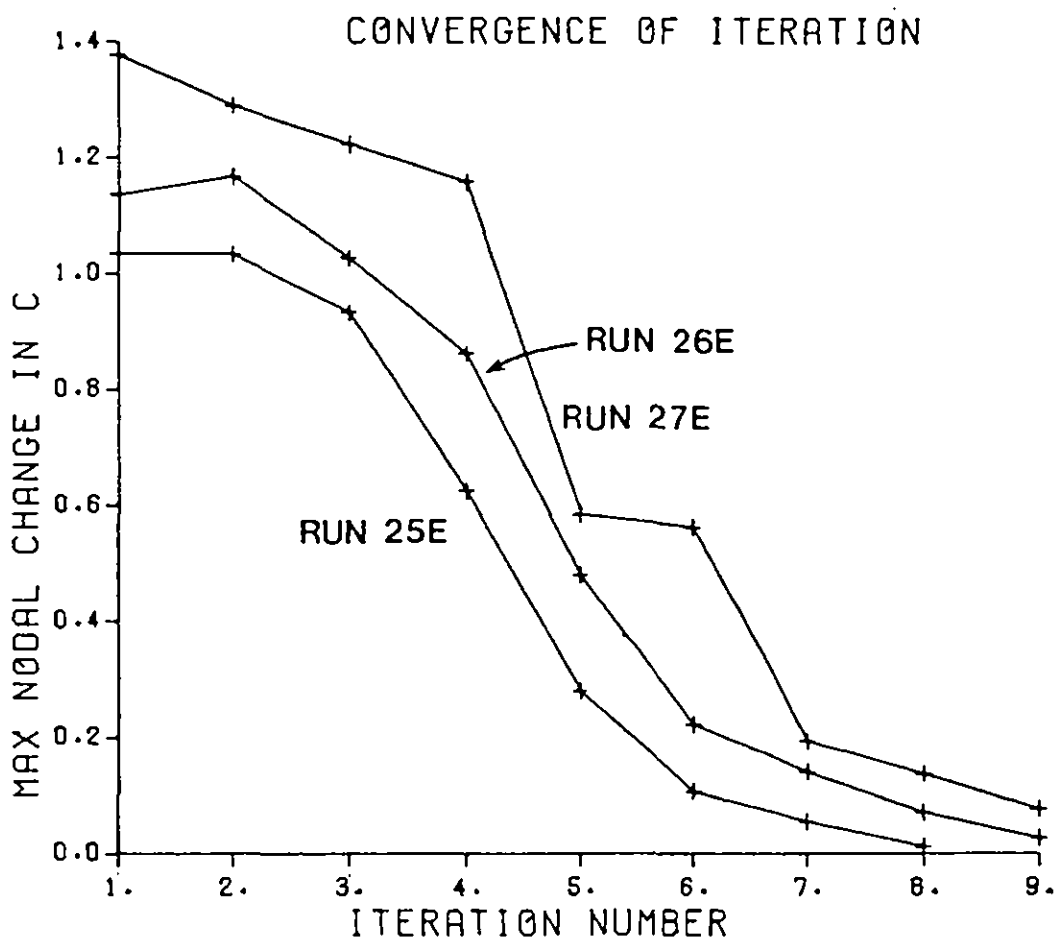


Figure 12

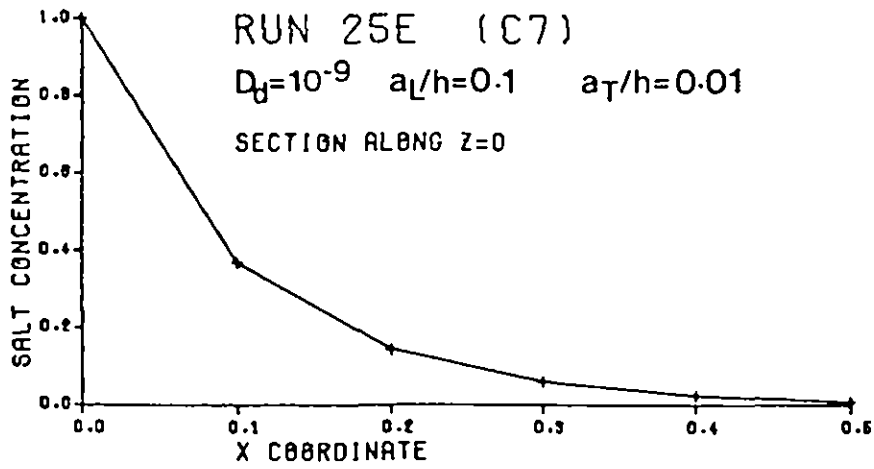


Figure 13

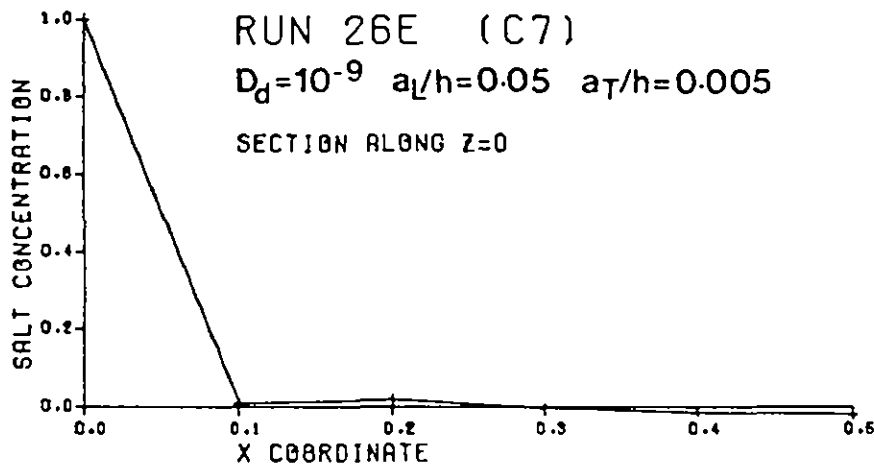


Figure 14

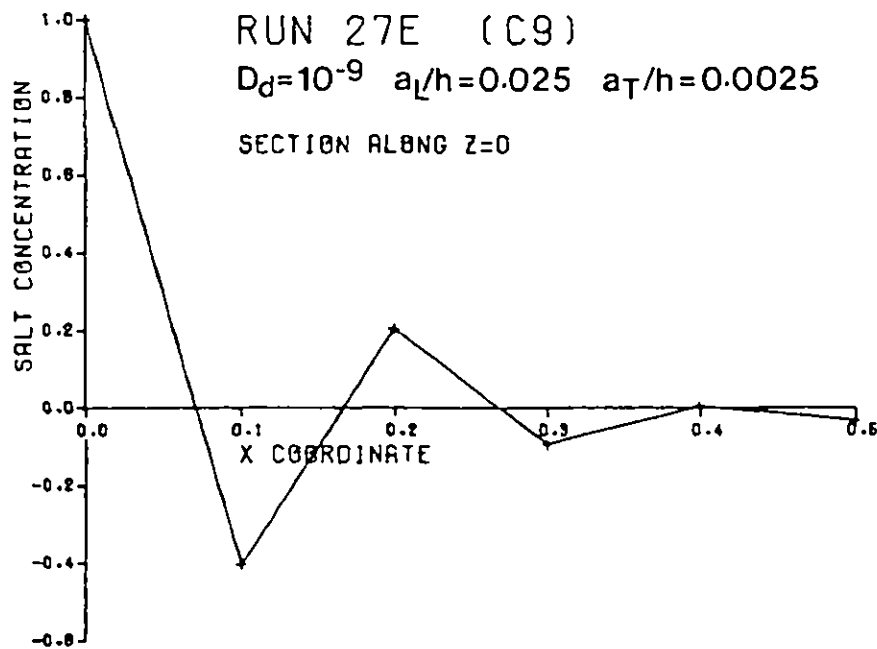


Figure 15

CONVERGED CONCENTRATION SOLUTIONS : $D_d = 10^{-9}$

RUN 25E [C7] ——— $a_L/h=0.1$ $a_T/h=0.01$

RUN 26E [C9] - - - - - $a_L/h=0.05$ $a_T/h=0.005$

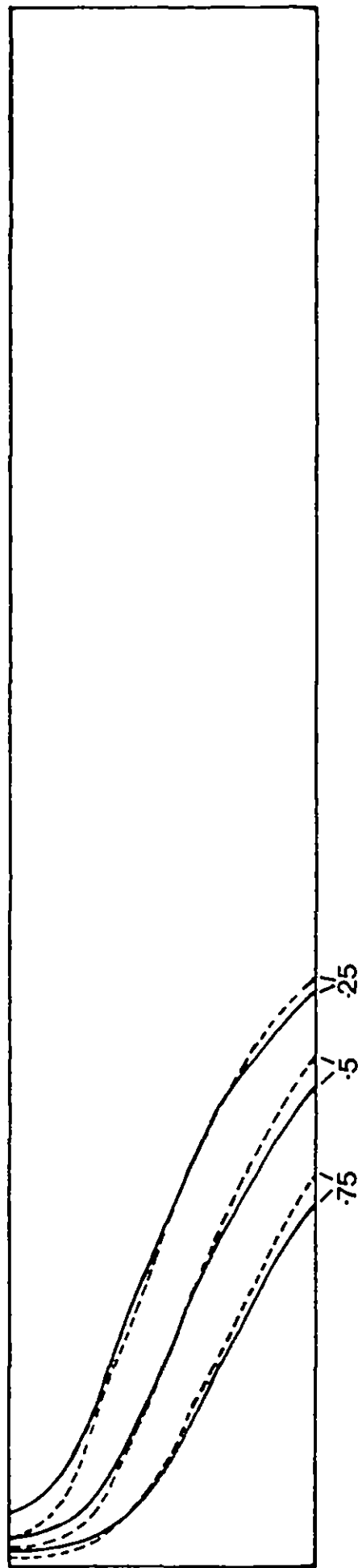


Figure 16

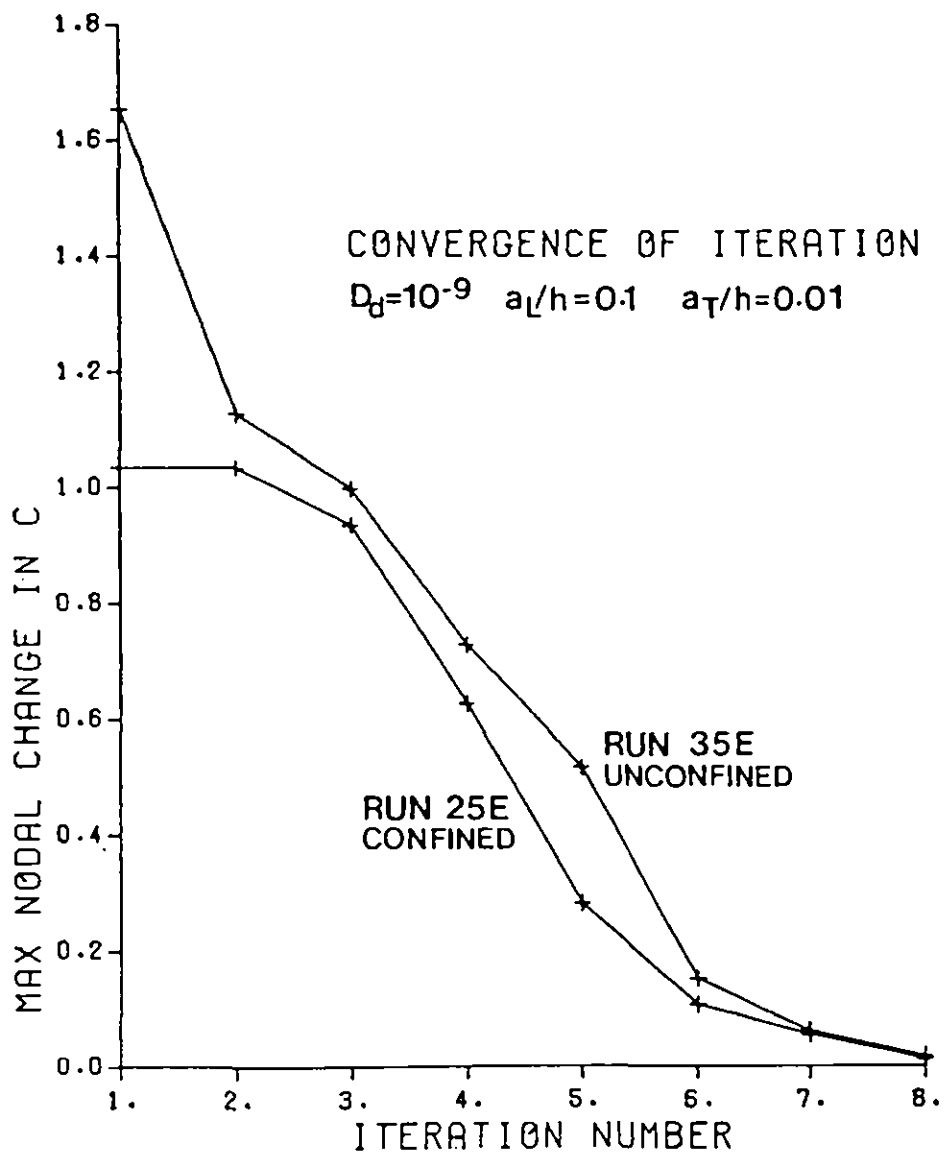


Figure 17

RUN 35E

CONVERGENCE OF ITERATION

$D_d = 10^{-9}$ $a_L/h = 0.1$ $a_T/h = 0.01$

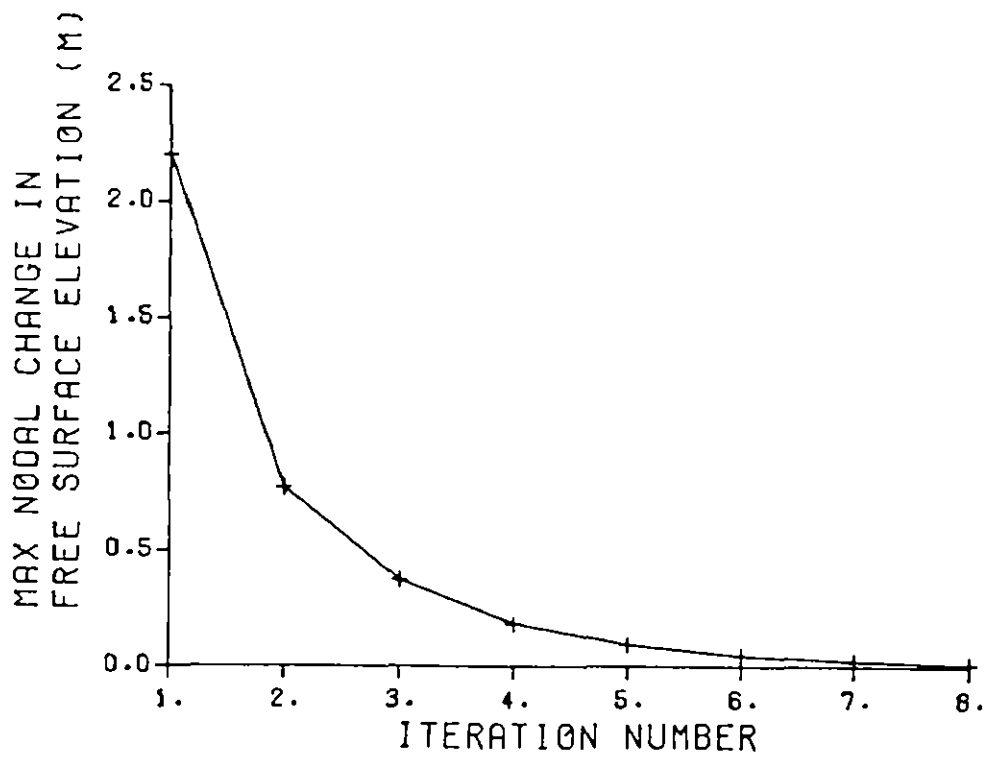


Figure 18

CONCLUSIONS

The convergence of the iterative scheme depends on a suitable choice of relaxation factor ω ; a value of $\omega = 0.5$ was found to give convergence over a wide range of parameter values, whereas with $\omega = 1.0$ the convergence was slower and was restricted to a very limited range of parameters.

Solutions have been obtained using both the full form of the mechanical dispersion tensor and an approximation which assumes that the flow is essentially horizontal resulting in a diagonal form for the mechanical dispersion tensor. This horizontal flow approximation was found to result in the 'toe' of the saline wedge extending further inland, although it has relatively little effect on the spacing of the isochlors.

A reduction in the longitudinal and transverse dispersivities, a_L and a_T , was found to result in the isochlors coming closer together; this effect is most marked at the top of the aquifer in the vicinity of the coast. Too great a reduction in a_L and a_T was found to give a solution for the salt concentration which exhibits spatial oscillations; further refinement of the finite element mesh should smooth out this oscillation.

The iterative scheme has been extended to cope with a free surface boundary at the top of the aquifer. The convergence of the position of this boundary was found to be more rapid than that of the concentration solution, and the overall increase in the number of iterations necessary for convergence was found to be small.

REFERENCES

- BEAR, J. - Hydraulics of Groundwater, McGraw-Hill, 1979
- HENRY, H.R. - Effects of dispersion on salt encroachment in coastal aquifers, U.S. Geological Survey Water Supply Paper 1613C, C70-C84, 1964
- NISHI, T.S., BRUCH, J.C. and LEWIS, R.W. - Movement of pollutants in a two-dimensional seepage flowfield, Journal of Hydrology, Vol 31, 307-321, 1976
- FRIND, E.O. - Seawater intrusion in continuous coastal aquifer-aquitard systems, Finite Elements in Water Resources, Eds. Wang, S.Y., Brebbia, C.A., Alonso, C.V., Gray, W.G. and Pinder, G.F., University of Mississippi, 1980
- WIKRAMARATNA, R.S. and WOOD, W.L. - On the coupled equations of the groundwater quality problem, Proc. Int. Conf. on Numerical Methods for Coupled Problems, Swansea, September 1981.
- VAN DYKE, M. - Perturbation Methods in Fluid Mechanics, Academic Press, 1964
- STRANG, G. and FIX, G.J. - An Analysis of the Finite Element Method, Prentice-Hall, 1973
- ZIENKIEWICZ, O.C. - The Finite Element Method, McGraw-Hill, 1977.
- WEAST, R.C., SELBY, S.M. and HODGMAN, C.D. - Handbook of Chemistry and Physics, 46th Edition, The Chemical Rubber Company, 1965

ACKNOWLEDGEMENTS

The author is grateful to the Director of the Institute of Hydrology, Dr J S G McCulloch for permission to use the computer facilities at the Institute to develop and run the programs and to prepare this report as part of his work at the Institute, Special thanks are due to Dr W L Wood of Reading University for advice and assistance throughout the project and to a number of colleagues at the Institute of Hydrology for their many helpful comments. Finally, the author would like to thank Sue Plinston for typing the manuscript.



Institute of Hydrology Wallingford Oxfordshire OX10 8BB UK
Telephone Wallingford (STD 0491) 38800 Telegrams Hycycle Wallingford Telex 849365 Hydrol G

The Institute of Hydrology is a component establishment of the Natural Environment Research Council